16TH EUROPEAN CONFERENCE ON EARTHQUAKE ENGINEERING THESSALONIKI 18 - 21 JUNE 2018

RESPONSE ANALYSES OF HIGH-RISE BUILDINGS TO VERY STRONG NEAR-SOURCE GROUND MOTIONS IN OSAKA, JAPAN

Yasuhiro Hayashi [1], Saki Ohmura [2], Mina Sugino [3]

ABSTRACT

The Uemachi fault belt runs right under Osaka city which is one of the biggest cities in Japan. Serious damage may occur in high-rise buildings due to strong pulse-like ground motions when the inland shallow earthquake occurs. The objective of this paper is to estimate the response and damage of high-rise buildings against strong near-source ground motions in Osaka, Japan.

First, we have collected information of almost all high-rise buildings in Osaka and analyzed the number of buildings according to completion years and building use. It is found that the number of condominium buildings has been increased and the number of the base-isolated condominium buildings was almost the same as that of the condominium buildings without base-isolation after 2006.

Next, we have constructed the stick models of steel or reinforced concrete buildings without base-isolation and base-isolated buildings. Then, we have conducted nonlinear response analyses varying the height of buildings. Against the design input ground motions (Level 3C), the maximum story shear deformation angle of buildings without base-isolation is around 0.01 - 0.03 rad. In contrast, the maximum story shear deformation angle of base-isolated buildings does not exceed 0.01 rad but almost all the existing base-isolated buildings may collide with retaining walls. Against the predicted earthquake ground motions (UMT33), the maximum story shear deformation angle of buildings is much larger than that against the design input ground motions.

Keywords: High-rise building; Base-isolated building; Near-source ground motion; Response analysis; MDOF shear model

1. INTRODUCTION

The Uemachi fault belt runs right under Osaka city which is one of the biggest cities in Japan. Serious damage may occur in high-rise buildings due to strong pulse-like ground motions when the inland shallow earthquake occurs.

On the other hand, response analyses of high-rise building to pulse-like ground motions have been conducted by various authors (Hall, et al. 1995; Alavi, et al. 2004; Sato et al. 2010; Alonso-Rodríguez, et al. 2015, and so on). Nevertheless, it is important to grasp the impact of ground motions peculiar to Uemachi fault belt on various size buildings. Therefore, the objective of this paper is to estimate the response and damage of high-rise buildings against strong near-source ground motions in Osaka, Japan. To achieve the objective, we collect information of almost all high-rise buildings in Osaka and analyze the number of buildings according to completion years and building use. Next, we construct stick models of steel or reinforced concrete buildings without base-isolation and base-isolated

[1] Professor, Department of Architecture and Architectural Engineering, Kyoto University, Kyoto, Japan, hayashi@archi.kyoto-u.ac.jp
[2] Graduate Student, Department of Architecture and Architectural Engineering, Kyoto University, Kyoto, Japan, rp-ohmura@archi.kyoto-u.ac.jp
[3] Assistant Professor, Department of Architecture and Architectural Engineering, Kyoto University, Kyoto, Japan, rp-sugino@archi.kyoto-u.ac.jp

buildings. Then, we conduct nonlinear response analyses varying the height of buildings. As input waves, we choose design input ground motions for the Uemachi fault belt earthquake in Osaka determined by industry-academia research group in Osaka. For comparison, earthquake ground motions for the Uemachi fault belt earthquake predicted by the municipal government and prefectural government of Osaka and typical observed near-fault ground motions are also used as input motions.

2. HIGH-RISE BUILDINGS IN OSAKA

In order to understand the influence of results of response analysis in Section 5, we develop the database of almost all high-rise buildings whose height is more than about 50m in Osaka and analyzed the number of buildings according to completion years and building use. The information of the buildings is collected based on websites of lists of high-rise buildings, websites of real estate, 3D view of Google earth and published structural design documents. Most of office buildings are steel structure and condominium buildings are RC structure.

Figure 1 (a) shows the transition of the number of buildings by building use. Before 1995, many office buildings were constructed, but after 1995 the number of office buildings have been decreased. On the other hand, condominium buildings began to be constructed in the first half of the 1980s and tended to increase until about 2010. Although it is somewhat declining after 2010, there still remains a large proportion of condominium buildings in the high-rise buildings. In addition, the total number of office buildings and condominium buildings amounts to 392 buildings, accounting for over 80%.

Figure 1 (b) shows the transition of the number of condominium buildings. In the Figure, we distinguish between buildings without base-isolation and base-isolated building. Base-isolated buildings have been completed since 2001. The number of base-isolated buildings completed after 2006 is almost the same as that of buildings without base-isolation.

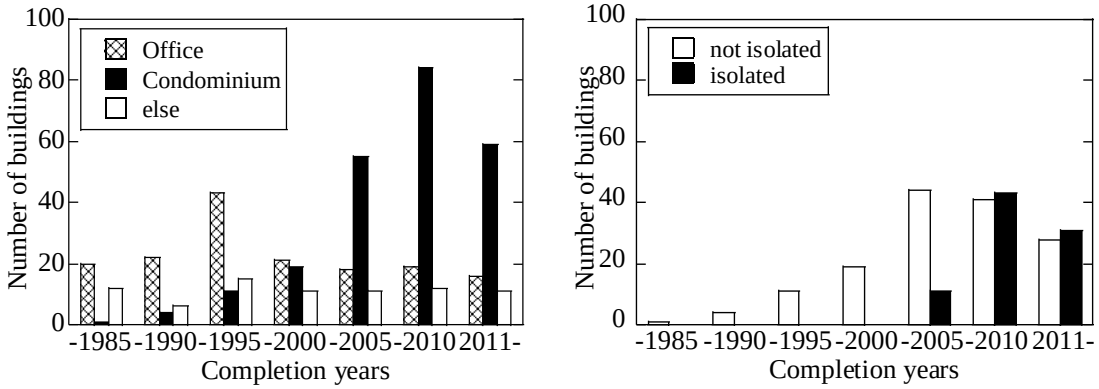

(a) Use (b) Condominium buildings

Figure 1. Transition of the number of super high-rise buildings

3. INPUT MOTIONS

As input motions for response analyses, we use design input ground motions and predicted earthquake ground motions for the Uemachi fault belt earthquake. For comparison, typical observed near-fault ground motions are also used.

Table 1 shows the list of input motions we use in this study. Figure 2 shows the velocity waveform. Figure 3 shows the pseudo-velocity response spectra ($_pS_v$ spectra). Figure 4 shows the displacement response spectra (S_d spectra). Damping ratio h of $_pS_v$ and S_d spectra is h=0.05. The response spectrum

of the seismic load prescribed by the notification of the Building Standard Law in Japan (BSL) are also shown in Figures 3 and 4. In this study, we define *pulse period* as the period when the ${}_pS_v$ spectrum is the peak value (Suzuki, et al. 2010). Figure 5 shows the zone division of the design input ground motions for the Uemachi fault belt earthquake in Osaka, which is explained below.

3.1 Design input ground motions

Structural-design engineers in Osaka have established an industry-government-academia research group to develop the design input ground motions to high-rise buildings for the earthquake due to the Uemachi fault belt (DAISHINKEN 2015). The design input ground motions are determined from the predicted ground motions for 35 scenario earthquakes simulated by the stochastic Green's functions method (Osaka Prefectural Government 2007). The predicted ground motions are calculated by municipal government and prefectural government of Osaka for the planning of countermeasures against earthquake disaster. The amplitude of ${}_pS_v$ of the design input ground motions is approximately 1.2 to 1.8 times of the seismic load prescribed by the notification of BSL.

The research group provides three levels of the ground motions; Level 3A, 3B and 3C. Level 3C is the strongest among the three levels. Moreover, the research group also provide two types of the ground motions; Flat type (type F) and Pulse type (type P). The design input ground motions differ according to zones as shown in Figure 5. The zone is divided based on the amplification characteristics of the ground, the distance from the Uemachi fault and so on. Fault lines of the Uemachi fault identified by Nakata et al. (2002) are shown as thick dotted line in Figure 5. The black circles in Figure 5 indicate the location of the high-rise buildings in Osaka city whose structural design documents are briefly published.

In this study, we use both type F and type P ground motions of Level 3C at A3 zone where a lot of high-rise buildings stand as shown in Figure 5. The PGV of 3C (type F) and 3C (type P) are about 120 cm/s and 150 cm/s, respectively, as shown in Figure 2 (a). The pulse period of 3C (type P) is clearly found at about 3 - 5 seconds, although that of 3C (type F) is not clear as shown in Figure 3 (a). The maximum values of the S_d spectra of Level 3C ground motions are more than 100 cm as shown in Figure 4 (a).

3.2 Predicted ground motions

The predict ground motions are calculated using a hybrid simulation technique using the stochastic Green's functions method and three-dimensional finite difference method. Among 35 scenario earthquakes mentioned above, the most serious scenario UMT33 is selected in order to estimate the maximum damage or loss in Osaka city. The rupture initiation point of the scenario UMT33 is the northern part of Osaka city that affects the severest to the buildings in the center of Osaka city. The ground motions which has the largest PGV during the scenario UMT33 earthquake are selected for input motions. The PGV of the input motion is about 360 cm/s as shown in Figure 2 (a). Pulse period is about 3-4 seconds and the peak of the ${}_pS_v$ spectrum exceeds more than 1000 cm/s as shown in Figure 3 (a). The peak values of S_d spectrum are more than 650 cm as shown in Figure 4 (a).

3.3 Observed ground motions

We use three observed ground motions of which the pulse periods differ each other. First, TAK is the NS component of the records at Takatori station during the 1995 Hyogo-ken Nambu, Kobe, earthquake by Railway Technical Research Institute. Second, NIS is the EW component of the records at Nishihara village office in Kumamoto prefecture during the 2016 Kumamoto earthquake (main shock) by Kumamoto prefectural government. Third, TCU068 is the EW component of the records at TCU068 station during the 1999 Chi-Chi earthquake by Central Weather Bureau (Taiwan). The PGV of TAK, NIS, and TSU068 are about 130 cm/s, 240 cm/s and 200 cm/s, respectively, as shown in Figure 2 (b). Figure 3 (b) indicates that TAK has two pulse periods around 1-2 seconds, NIS has two pulse periods of about 0.8 and 3 seconds and TCU068 has one pulse period which is about 9 seconds.

Table 1. List of input motions

Name	Use	Earthquake	Site
3C (Type P)	Design wave	Uemachi fault	Zone A3 (see Figure 5)
3C (Type F)			
UMT33	Predicted		Site where PGV is the largest
TAK	Observed	1995 Kobe EQ. (Japan)	Takatori station
NIS		2016 Kumamoto EQ. (Japan)	Nishihara town office
TCU068		1999 Chi-Chi EQ. (Taiwan)	TCU068 station

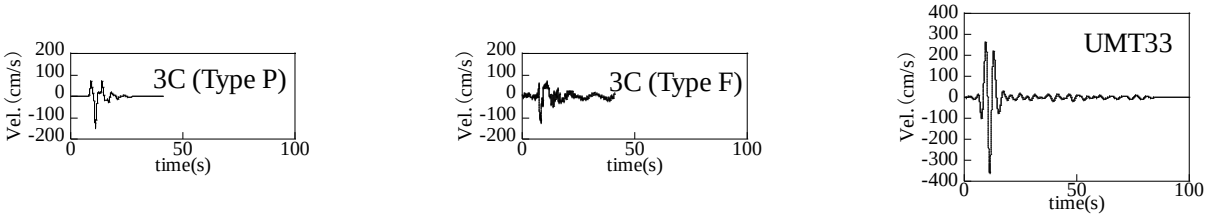

(a) Design input ground motions of zone A3 and predicted ground motion UMT33

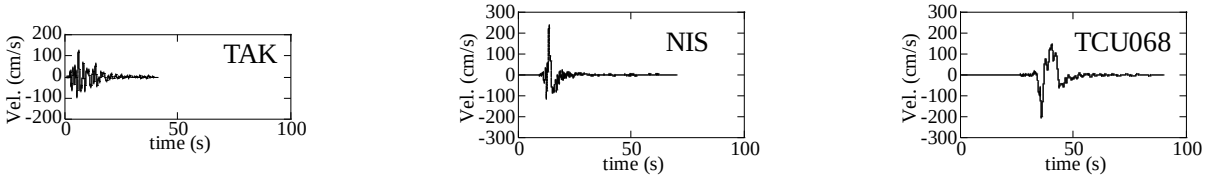

(b) Observed near fault ground motions

Figure 2. Input ground motions

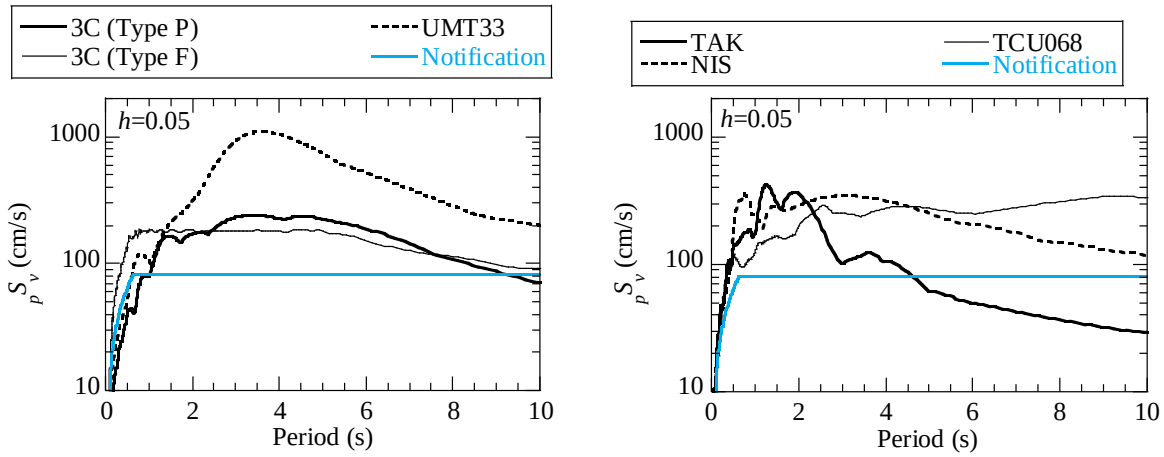

(a) Design ground motions (Uemachi fault)

(b) Observed near fault ground motions

Figure 3. Pseudo-velocity response spectra (h=0.05)

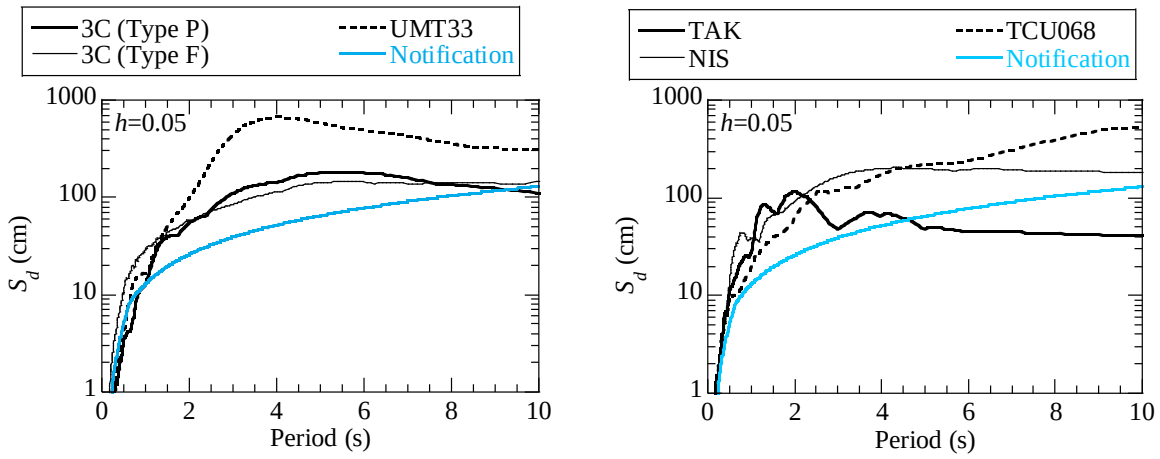

(a) Design ground motions (Uemachi fault) (b) Observed near fault ground motions

Figure 4. Displacement response spectra (h=0.05)

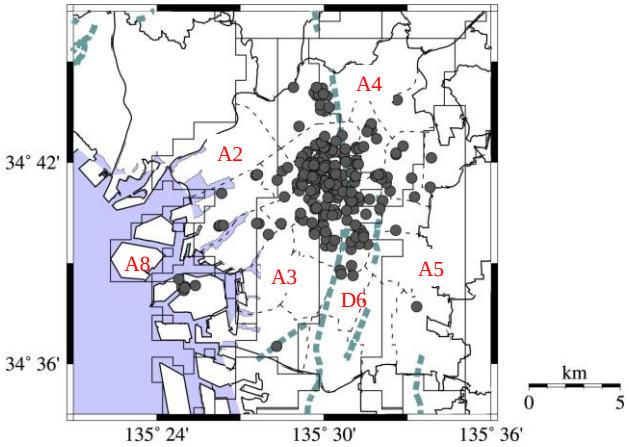

Figure 5. Zone division of the design input ground motions for the Uemachi fault belt earthquake in Osaka

4. BUILDING MODEL FOR RESPONSE ANALYSES

The stick models (MDOF shear models) are used for nonlinear response analyses for simplicity. In this section, we construct the models of which height H is selected as analysis variable. The parameters used in our model are shown in Table 2.

4.1 Buildings without base-isolation

We explain the models of steel buildings and reinforced concrete (RC) buildings without base-isolation. In our model, we change the height H every 12 m; the steel buildings are changed from 48 m to 300 m and the RC buildings are changed from 48 to 204 m. Fundamental natural period T_1 of the buildings is given by Equation 1.

$$T_1 = \gamma H \tag{1}$$

where γ is 0.025 for steel buildings and 0.02 for RC buildings as shown in Figure 6. In Figure 6, the relationship between the height and fundamental natural period of response analysis model of buildings, which are found in published structural design documents, are found also shown as dots.

The design base shear coefficient C_B is given by Equation 2.

$$C_B = C_0 R_t \tag{2}$$

where R_t is the vibration characteristic coefficient and the value of the soil profile type 2 (medium soil) of BSL is used as R_t in this study. The C_0 of steel buildings is 0.3 and RC buildings is 0.2.

The stiffness distribution is linear and the stiffness ratio of the first story to highest story is three to one. The floor weight and story height of each model is constant according as structural type as shown in Table 2. From the fundamental natural period T_1 and the stiffness distribution, the initial stiffness K_1 at the first story is calculated.

The restoring force characteristics of the first story is as shown in Figure 8. Normal tri-linear restoring force characteristics are used for steel buildings, and degrading tri-linear type are used for RC buildings. Note that the shape of the restoring force characteristics is determined based on Mayahara et al. (2005) and Akita et al. (2014). The deformation angle R_1 and R_2 in Figure 8 are calculated from the design base shear coefficient C_B, the initial stiffness K_1 and the weight of the model. The restoring force characteristics of the other stories are proportional to that of the first story. The damping type is tangent stiffness-proportional damping and the damping ratio is shown in Table 2.

4.2 Base-isolated buildings

The superstructures of base-isolated buildings are modeled the same way as the RC buildings without base-isolation mentioned above. We assume at Equation 1 that T_1 is the fundamental natural period when the isolator is fixed and H is the height of the superstructure as shown in Figure 7 (a). In Figure 7, buildings, whose structural design documents are published briefly, are also shown as black circles.

In order to develop models for two types of superstructures which is RC frame and RC frame with shear walls, we use two types of the restoring force characteristics of the model as shown in Figure 8.

Next, we explain about the model of the isolator. The stiffness of the isolator k_e is linear and given by Equation 3 and 4.

$$T_e = 0.025H + 3 \tag{3}$$

$$k_e = M\left(2\pi / T_e\right)^2 \tag{4}$$

where M is the total mass of a building. The T_e is the equivalent fundamental natural period for the deformation of the isolator when level 2 ground motion of BSL is input. Note that the mass of the isolator is twice that of each story of the superstructure. Equation 3 is determined from Figure 7 (b) which describes the relationship between T_e and H. The type of damping is viscous damping and the damping factor c_e is given by Equation 5.

$$c_e = 2h_e\sqrt{Mk_e} \tag{5}$$

where h_e is the damping ratio and h_e=0.2 in this study.

Figure 9 shows the range of isolator movement of the base-isolated buildings in Osaka city of which published structural design documents are found. It turns out that many of the rage of isolator movement are distributed over the range of 60 to 90 cm.

Table 2. Parameters used in the building models

	Steel	RC, Base-isolated
γ	0.025	0.02
C_0	0.3	0.2
Floor height (m)	4	3
Height H (m)	48~300	48~204
Weight per unit area (kN/m^2)	0.8 x 9.8	9.8
Plane area of each floor (m^2)	900	
Damping ratio	0.02	0.03

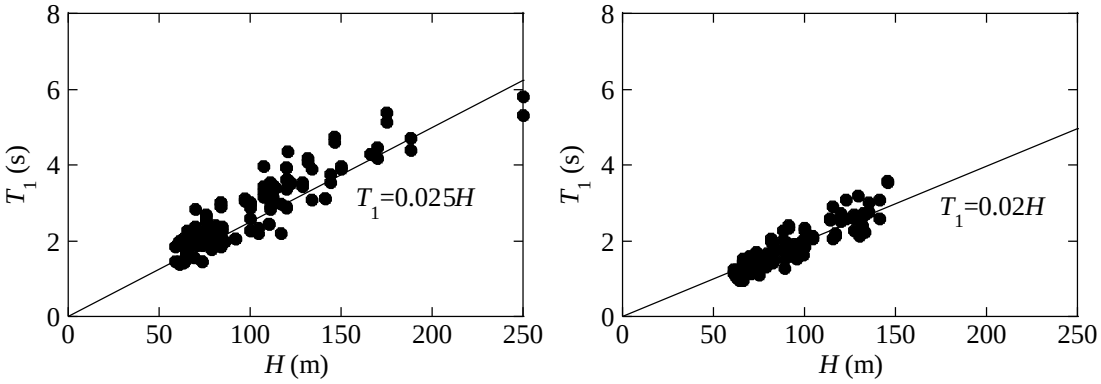

(a) Steel (b) RC

Figure 6. Fundamental natural period except for base isolated buildings

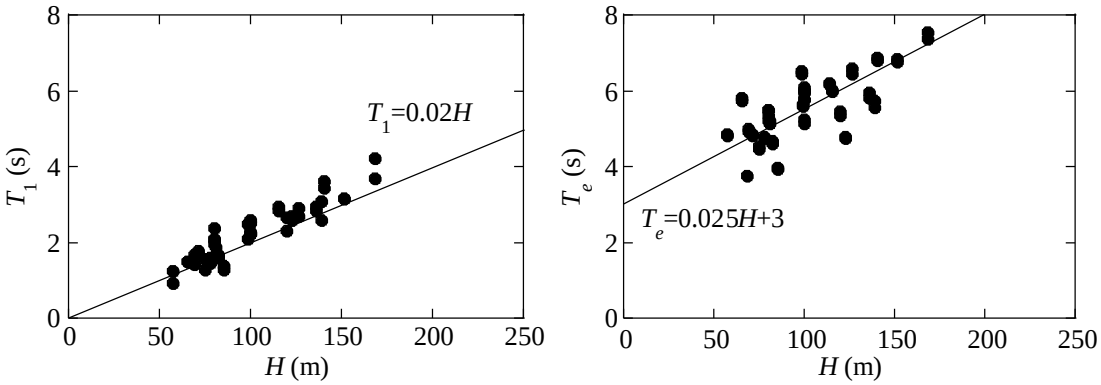

(a) Isolator is fixed (b) Equivalent natural period for Level 2

Figure 7. Fundamental natural period of base isolated buildings

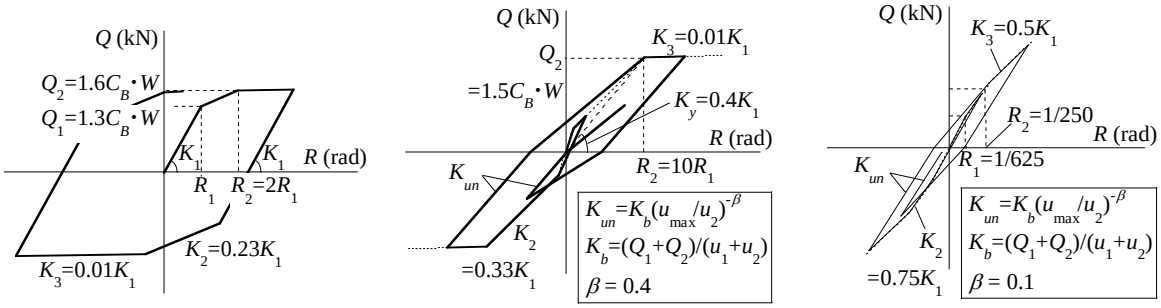

(a) Steel structure (b) RC frame (c) RC frame with shear walls

Figure 8. Restoring force characteristics

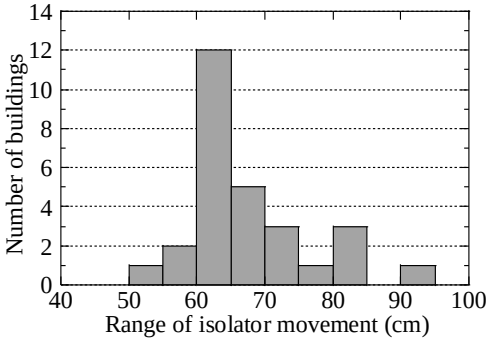

Figure 9. Range of isolator movement of base isolated buildings

5. RESULTS OF ANALYSES

In this section, we describe the results of nonlinear response analyses varying the height H of buildings. The R_{max} is calculated from the maximum story deformation angle among all stories of the building and is associated with the damage of superstructures. The D_{max} is the maximum deformation of the isolator and is associated with the collision of the buildings with the retaining walls. Collision occurs in all base-isolated buildings because the range of the isolator movement of almost buildings in Osaka city is smaller than 100 cm as shown in Figure 9. Figures 10 - 15 show the result of the analyses.

Figure 10 shows that R_{max} of the buildings without base-isolation against the design input ground motions (Type P and F of Level 3C) and the predicted ground motion (UMT33). The maximum story deformation angle R_{max} of both the steel and RC buildings against both 3C (type P) and 3C (type F) is around 0.01 - 0.03 rad. The R_{max} against 3C (type P) is larger than that against 3C (type F) when the height H is higher than about 100 m. The R_{max} against 3C (type P) is about 0.03 rad when H is around 100 - 150 m and R_{max} decreases according to H increases when H is higher than 150 m. The R_{max} against UMT33 is much larger than that against the design input ground motions and severe although R_{max} decreases according to H increases. Figures 11 and 12 show R_{max} and D_{max} of the base-isolation buildings, respectively, against 3C (type P), 3C (type F) and UMT33. The D_{max} of RC frame is smaller than that of RC frame with shear walls although R_{max} of RC frame is larger than that of RC frame with shear walls. Especially in RC frame with shear walls, D_{max} against both 3C (type P) and 3C (type F) is very large and is nearly 100 cm although R_{max} is smaller than 0.01 rad. Against UMT33, not only D_{max} but also R_{max} is very large that R_{max} far exceeds 0.01 rad.

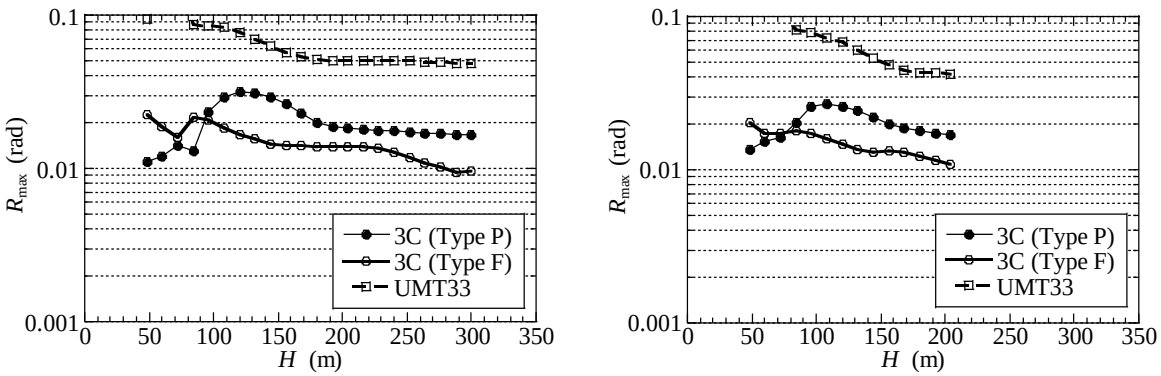

(a) Steel buildings (b) RC buildings

Figure 10. R_{max} of buildings without base-isolation (design input ground motions and predicted ground motion)

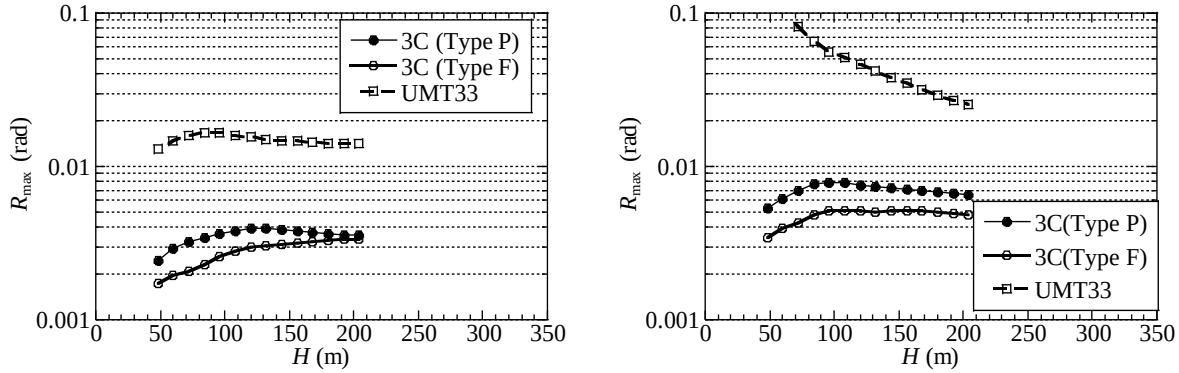

(a) RC frame with shear walls (b) RC frame

Figure 11. R_{max} of base-isolated buildings (design input ground motions and predicted ground motion)

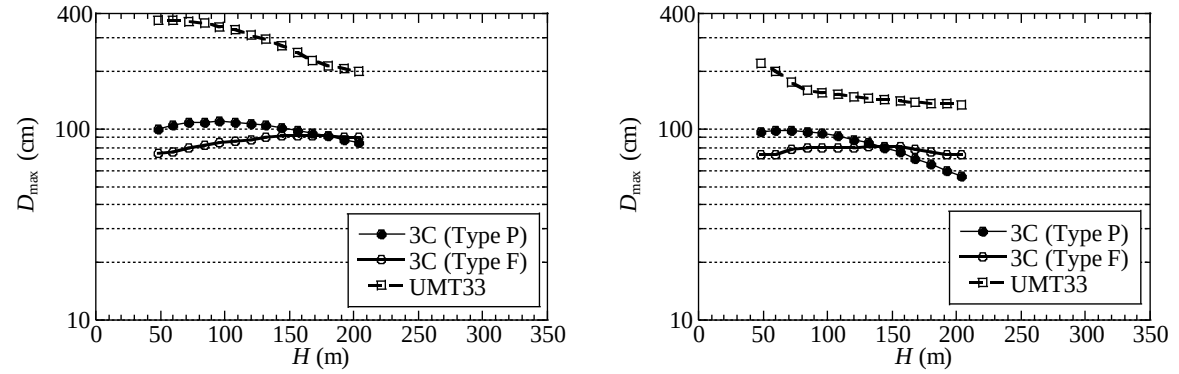

(a) RC frame with shear walls (b) RC frame

Figure 12. D_{max} of base-isolated buildings (design input ground motions and predicted ground motion)

Figure 13 shows the R_{max} of the buildings without base-isolation against the observed ground motions. Tendency of the relationship between R_{max} and H does not change by structural type. As shown in Figure 13 (a), R_{max} is decreasing with the increase in H against TAK which has pulse periods around 1-2 seconds. On the contrary, R_{max} is the maximum when H is around 100 - 150 m against NIS and R_{max} is the maximum when H is more than 150 m against TCU068. The result indicates that H at which R_{max} is the largest increase with the pulse periods of pulse-like ground motions.

Figure 14 shows R_{max} and Figure 15 shows D_{max} of the base-isolation buildings against the observed ground motions. Both R_{max} and D_{max} of both RC frame and RC frame with shear walls is the largest against TCU068. The result is assumed to be related to Figures 3 and 4 that ${}_pS_v$ and S_d spectra are the largest among the three ground motion more than 4 seconds.

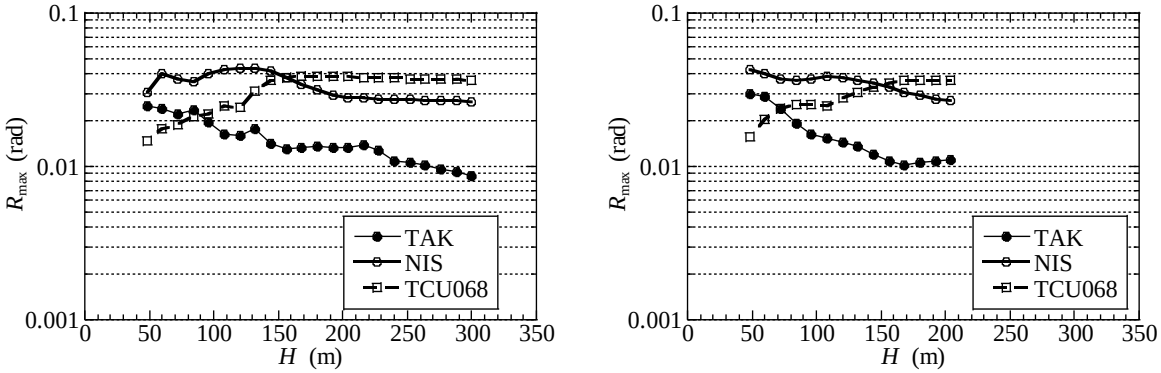

(a) Steel buildings (b) RC buildings

Figure 13. Variation in R_{max} of buildings without base-isolation (observed ground motions)

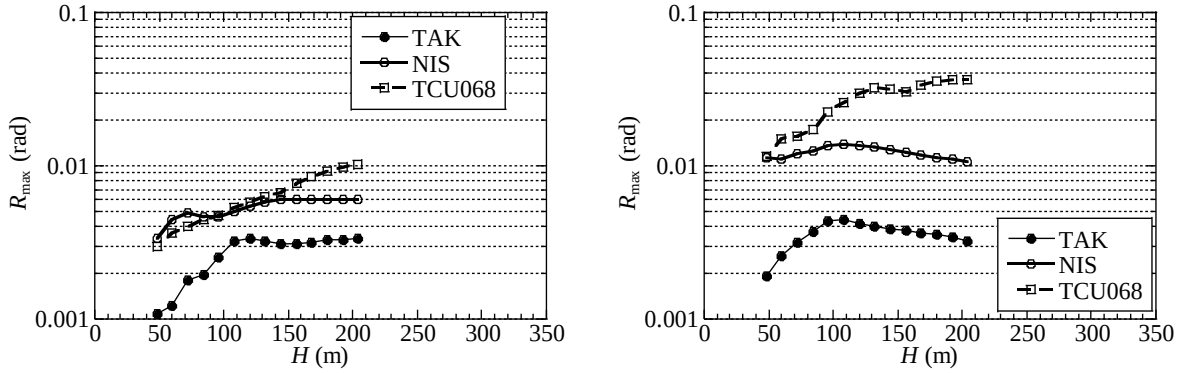

(a) RC frame with shear walls (b) RC frame

Figure 14. R_{max} of base-isolated buildings (observed ground motions)

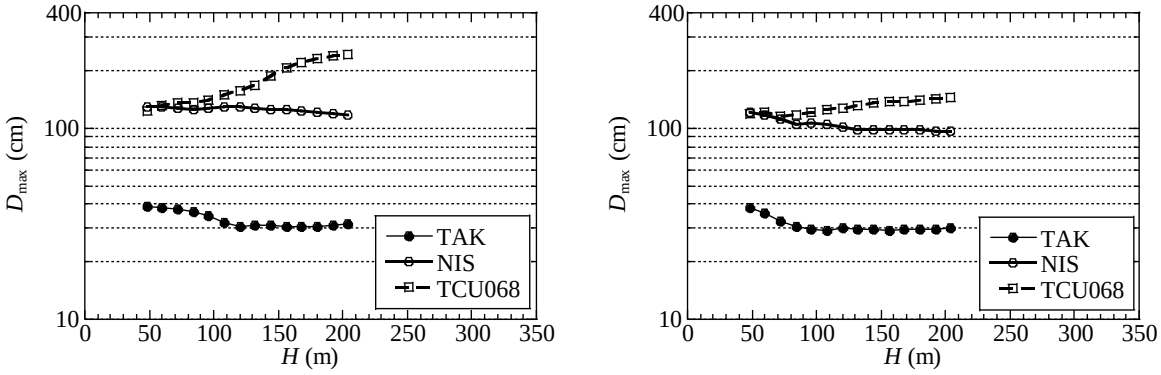

(a) RC frame with shear walls (b) RC frame

Figure 15. D_{max} of base-isolated buildings (observed ground motions)

6. CONCLUSIONS

The objective of this paper is to estimate the response and damage of high-rise buildings against strong near-source ground motions in Osaka, Japan. To achieve the objective, we have collected information of almost all high-rise buildings in Osaka and analyzed the number of buildings according to completion years and building use. Moreover, we have constructed stick models of steel or reinforced

concrete buildings without base-isolation and base-isolated buildings. Then, we have conducted nonlinear response analyses varying the height of buildings. As input waves, we chose the design input ground motions (Level 3C) and the predicted earthquake ground motions (UMT33) for the Uemachi fault belt earthquake in Osaka. For comparison, typical observed near-fault ground motions are also used as input motions.

As results of this study, the following conclusions have been drawn.

(a) The number of condominium buildings has been increased and the largest number of building was condominium buildings after 2001. Base-isolated condominium buildings have been constructed since 2001 and the number of the base-isolated condominium buildings was almost the same as that of the condominium buildings without base-isolation after 2006.

(b) Against the design input ground motions (Level 3C), the maximum story shear deformation angle of buildings without base-isolation is around 0.01 - 0.03 rad. In contrast, the maximum story shear deformation angle of base-isolated buildings does not exceed 0.01 rad but almost all the existing base-isolated buildings may collide with retaining walls.

(c) Against the predicted earthquake ground motions (UMT33), the maximum story shear deformation angle of buildings without base-isolation is much larger than that against the design input ground motions. The maximum story shear deformation angle of base-isolated buildings is also so large that far exceeds 0.01 rad.

(d) The height of the building at which the maximum response is the largest increases with the pulse periods of pulse-like ground motions.

7. ACKNOWLEDGMENTS

The authors would like to thank Japan Structural Association of Kansai, Osaka prefectural government Railway Technical Research Institute, Kumamoto prefectural government and Central Weather Bureau (Taiwan) for providing ground motion data. The authors also would like to thank Rie Okazawa for helping to conduct the response analyses.

8. REFERENCES

Hall JF, Heaton TH, Halling MW, Wald DJ (1995). Near-Source Ground Motion and its Effects on Flexible Buildings. *Earthquake Spectra*, 11(4): 569-605.

Alavi B, Krawinkler H (2004). Behavior of Moment-Resisting Frame Structures subjected to Near-Fault Ground Motions. *Earthquake Engineering & Structural Dynamics*, 33(6): 687-706.

Sato K, Su Z, Kawabe H, Suita K, Hayashi Y (2010). Building Response of Highrise Building to Ground Motion Predicted for Uemachi Faults. AIJ Journal of Technology and Design, 16(33), 463-468. (in Japanese)

Alonso-Rodríguez A, Miranda E (2015). Assessment of Building Behavior under Near-Fault Pulse-Like Ground Motions through Simplified Models. *Soil Dynamics and Earthquake Engineering*, 79: 47-58.

Suzuki K, Kawabe H, Yamada M, Hayashi Y (2010). Design Response Spectra for Pulse-like Ground Motions. *Journal of Structural and Construction Engineering (Transactions of AIJ)*, 75(647): 49-56. (in Japanese)

Osaka Prefectural Government (2007). Report of Study about Comprehensive Disaster Mitigation (Estimation of Earthquake Damage) in Osaka Prefecture. (in Japanese)

Research Group about Design Earthquake Ground Motion and Design Method of Building for Inland Earthquake underneath the Osaka Area, commonly called DAISHINKEN (2015). Design Earthquake Ground Motion and Aseismic Design Guideline of Building for Inland Earthquake underneath the Osaka Area, *JSCA Kansai: http://jscakansai.com/*. (in Japanese)

Nakata T, Imaizumi T (2002). Detailed Digital Map of Active Faults (Product Serial Number: DAFM1240). *University of Tokyo Press*. (In Japanese)

Mayahara T, Kitamura H (2005). Existing Steel High-Rise Buildings Subjected to the Long-Period Ground Motions: Part 1 Seismic Evaluation Based on Time-History Analysis. *Summaries of technical papers of annual meeting Architectural Institute of Japan*, Structure III: 565-566. (in Japanese)

Akita T, Ishizuka K, Fujiwara M, Izumi N (2014). Distribution of Seismic Capacity Index Related to Ultimate Limit of Existing High-rise RC Buildings, *Proceedings of the Japan Concrete Institute*, 36(2): 643-648. (in Japanese)